Stem Cell Reports
Article

ISSCR

OPEN ACCESS

Fast Generation of Functional Subtype Astrocytes from Human Pluripotent Stem Cells

Xiang Li,[1,5] Yezheng Tao,[1,5] Robert Bradley,[1,5] Zhongwei Du,[4,5] Yunlong Tao,[1] Linghai Kong,[1] Yi Dong,[1] Jeffrey Jones,[1] Yuanwei Yan,[1] Cole R.K. Harder,[1] Lindsay Morgan Friedman,[1] Magd Bilal,[1] Brianna Hoffmann,[1] and Su-Chun Zhang[1,2,3,4,*]

[1]Waisman Center, University of Wisconsin, Madison, WI 53705, USA
[2]Department of Neuroscience, School of Medicine and Public Health, University of Wisconsin, Madison, WI 53705, USA
[3]Department of Neurology, School of Medicine and Public Health, University of Wisconsin, Madison, WI 53705, USA
[4]BrainXell, Inc., Madison, WI 53711, USA
[5]Co-first author
*Correspondence: suchun.zhang@wisc.edu
https://doi.org/10.1016/j.stemcr.2018.08.019

SUMMARY

Differentiation of astrocytes from human pluripotent stem cells (hPSCs) is a tedious and variable process. This hampers the study of hPSC-generated astrocytes in disease processes and drug development. By using CRISPR/Cas9-mediated inducible expression of NFIA or NFIA plus SOX9 in hPSCs, we developed a method to efficiently generate astrocytes in 4–7 weeks. The astrocytic identity of the induced cells was verified by their characteristic molecular and functional properties as well as after transplantation. Furthermore, we developed a strategy to generate region-specific astrocyte subtypes by combining differentiation of regional progenitors and transgenic induction of astrocytes. This simple and efficient method offers a new opportunity to study the fundamental biology of human astrocytes and their roles in disease processes.

INTRODUCTION

Astrocytes are functionally indispensable for normal brain activities (Barres, 2008; Ullian et al., 2001; Zhang, 2001). Astrocytes play critical roles for the establishment and maintenance of functional neural networks through refining synapses, coordinating neuronal firing, maintaining the blood-brain barrier, as well as structural and metabolic support (Iadecola and Nedergaard, 2007; Sofroniew and Vinters, 2010; Ullian et al., 2001). Functional loss or impairment of astrocytes is implicated in a wide range of pathological processes and neural disorders, including Alzheimer's disease, Huntington's disease, amyotrophic lateral sclerosis, and epilepsy (Molofsky et al., 2012; Scuderi et al., 2013; Sofroniew and Vinters, 2010). In humans, astrocytes display unique hominid features (Oberheim et al., 2009). Human astrocytes are morphologically larger, structurally more complex, and functionally more diverse than those in the rodent brain (Oberheim et al., 2009; Robertson, 2014). The complexity of human astrocytes allows for the increased functional competence of the adult human brain (Oberheim et al., 2009; Robertson, 2014; Vasile et al., 2017). Thus, access to human astrocytes will substantially enable studies on the biology and pathology of astrocytes and facilitate therapeutic development.

Astrocytes have been successfully generated from human pluripotent stem cells, including embryonic stem cells (ESCs) and induced pluripotent stem cells (iPSCs) (Emdad et al., 2012; Hu et al., 2010; Krencik et al., 2011; Mormone et al., 2014; Roybon et al., 2013; Palm et al., 2015; Shaltouki et al., 2013; Tcw et al., 2017; Zhou et al., 2016) (Table S1). These methods are based on developmental principles to expand the neural progenitors until gliogenesis (Steinbeck and Studer, 2015; Tao and Zhang, 2016). Hence, the differentiation process ranges from 3 to 6 months. There are reports on astrocyte generation in a shorter time but the identity and functional properties of the astrocytes are less rigorously examined (Table S1). The main reason for this long process is that we lack effective ways to promote the gliogenic program of the neural progenitors and, as a result, wait for the progenitors to become gliogenic by "default." Such an approach also results in variations in the differentiated products.

One way to accelerate the differentiation process is to force the expression of cell-type-specific transcription factors in stem cells. This has been demonstrated by fast (2–4 weeks) generation of functional neurons from human ESCs (hESCs) through virus-mediated expression of a proneural gene, *Ngn2* (Zhang et al., 2013). In this study, using a similar strategy, we created hESC and iPSC lines with inducible expression of gliogenic transcription factors *NF1A* or *NF1A* plus *SOX9* via CRISPR/Cas9. Utilizing inducible expression of *NF1A* or *NF1A* plus *SOX9*, we developed a method for fast generation of homogeneous functional and transplantable astrocytes from hESCs and iPSCs in 4–7 weeks. Importantly, by patterning with morphogens during the induction, we developed a method to generate region-specific subtype astrocytes in the same time frame.

This is an open access article under the CC BY-NC-ND license (http://creativecommons.org/licenses/by-nc-nd/4.0/).

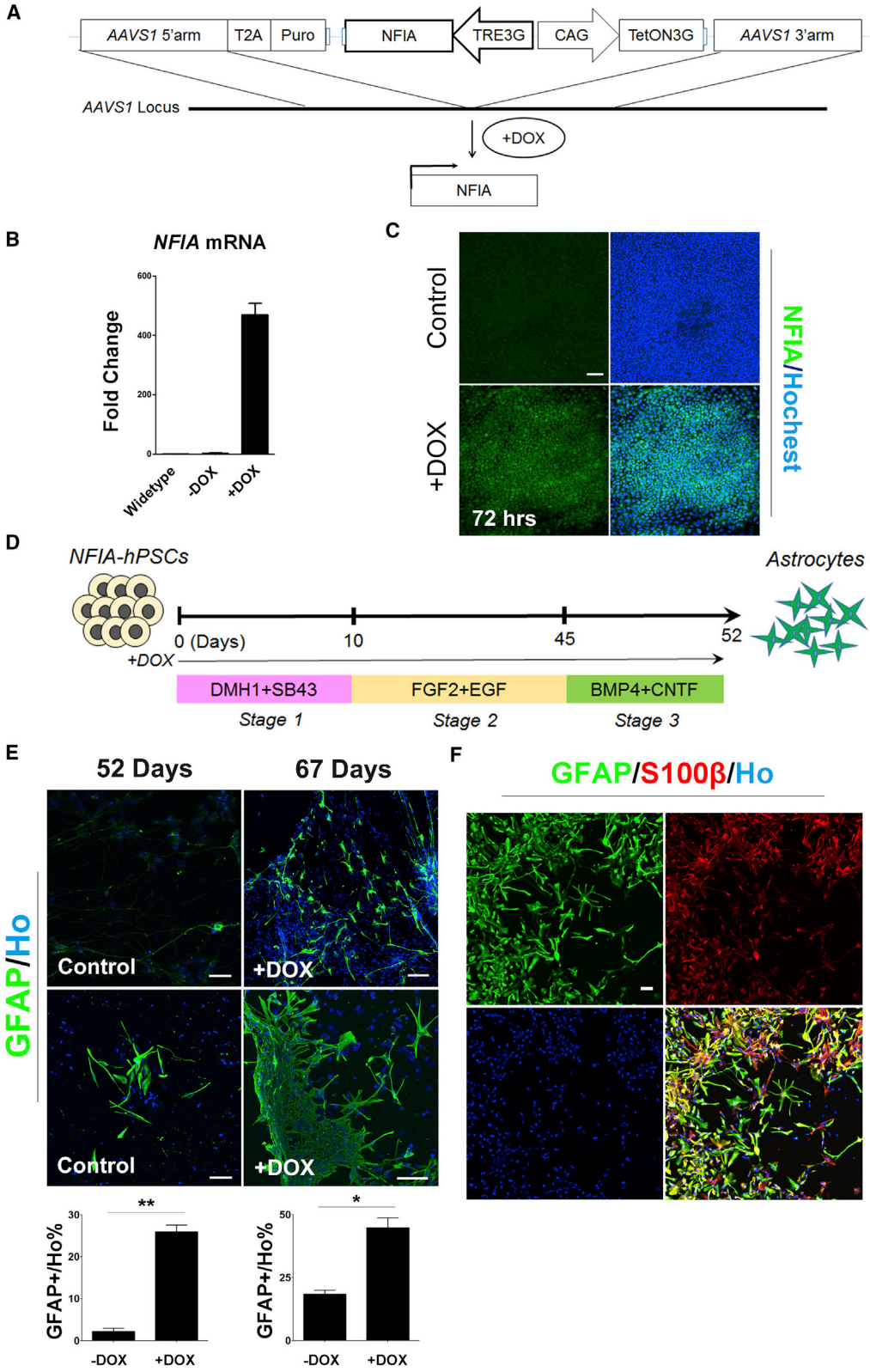

(legend on next page)

RESULTS

Expression of *NFIA* Facilitates Astrocyte Differentiation from hPSCs

The *NFI* (nuclear factor I) family transcription factors are crucial for the initiation of gliogenesis and acquisition of gliogenic competence in the developing CNS (Deneen et al., 2006; Kang et al., 2012; Miller and Gauthier, 2007; Tsuyama et al., 2015; Vong et al., 2015). To determine if *NFI* promotes astrocyte differentiation from human stem cells, we established hESC lines with inducible expression of *NFIA*. This was achieved by targeting TRE3G-*NFIA* in the AAVS1 locus by CRISPR/Cas9 (Qian et al., 2014) (Figure 1A). After drug selection and PCR verification, colonies were grown and cultured >3 passages before being subjected to induced expression of *NFIA* by adding doxycycline (DOX). Upon induction with DOX for 72 hr, *NFIA* mRNA and protein were robustly expressed, as indicated by qRT-PCR (Figure 1B) and immunocytochemistry (Figure 1C).

Previously, we developed the method of directed differentiation of hPSCs into astrocytes, in which GFAP-expressing astrocytes begin to appear at around 3 months and reach a peak at 6 months (Krencik et al., 2011). In this method, the hPSCs were committed in monolayer culture into the neural fate by SMAD inhibition as stage 1, then the cells were floated as neural progenitors in culture with fibroblast growth factor-2 (FGF-2) and epidermal growth factor (EGF) for as long as 5–6 months for the neural-to-glia developmental fate switch as stage 2, and plated down for astrocytic maturation as stage 3. To determine the effect of *NFIA*, we used the same differentiation scheme but with induced *NFIA* expression from the start of differentiation by DOX, and then subjected the induced cells to a 7-day maturation (Figure 1D). By weekly examination in stage 2, we found that about 20% GFAP+ cells were generated at 45 days of induction plus a 7-day maturation (Figures 1E and 1F). In contrast, the control group (without DOX) generated less than 3% GFAP+ astrocytes (Figure 1E). By extending the induction to 67 days, the GFAP+ cell population was further increased to 40%–50%, and the cells were larger with more processes than the induced cells at day 52 (Figure 1E). The astrocytic identity was further confirmed by its co-expression with S100β, another astrocyte-associated gene (Figure 1F). These results indicate that *NF1A* expression substantially speeds up the astrocyte differentiation from hESCs.

Expression of *NFIA* and *SOX9* Further Accelerates Astrocyte Differentiation

Besides *NFIA*, *SOX9* is another determining factor for the astroglial cell fate (Kang et al., 2012; Stolt et al., 2003; Vong et al., 2015). *NFIA* and *SOX9* form a complex to coordinate a transcriptional regulatory cascade for initiating gliogenesis during neural development (Kang et al., 2012). Astrocytic fates can be induced from neural progenitor cells *in vivo* or from cultured mouse fibroblasts by overexpressing *NFI* + *SOX9* (Gaiazzo et al., 2015). To determine if the combination of *NFIA* and *SOX9* further accelerates the astrocyte differentiation, we generated hESC lines with inducible expression of *NFIA* and *SOX9* by targeting the Tet3G-*NFIA* + *SOX9* into the AAVS1 locus using the same approach (Figure 2A). Again, the mRNA and protein of both genes were reliably induced by DOX (Figures 2B and S1A). Western blotting indicated that NFIA expression was higher in the NFIA + SOX9 line than the NFIA line (Figure S1C). This result is consistent with the previous report that NFIA expression is regulated and reinforced by SOX9 to coordinate a transcriptional regulatory cascade for the initiation of gliogenesis (Kang et al., 2012). Quantification of the immunostained cells showed that over 90% of the cells expressed either NFIA or SOX9, indicating that the vast majority of the cells co-expressed NFIA and SOX9 (Figures 2C and S1B).

The astrocyte induction and maturation was performed in the same way as for *NFIA* lines (Figure 2D). After 37 days' induction, around 30% of the cells became GFAP+ (Figure S1D). With extended (52 days) induction of *NF1A* and *SOX9*, 70%–80% of the cells became GFAP+ (Figure 2E). The astrocytic identity of the induced cells was confirmed by their co-expression of GFAP and S100β (Figure 2E). The efficiency and identity of the induced cells were reproducible using different engineered hESC clones (Figure S1E). Thus, expression of *NF1A* and *SOX9* results

Figure 1. Astrocyte Differentiation Induced by NFIA Expression

(A) Schematic depiction of the strategy for constructing and targeting TRE3G-*NFIA* into the AAVS1 locus.

(B) qRT-PCR analysis of induced expression of *NFIA*. n = 3 replicate reactions.

(C) Immunostaining analysis of induced expression of *NFIA*. Scale bar, 200 μm.

(D) Diagram of the facilitated generation of astrocytes by *NFIA* induction. Stage 1, neural fate commitment by dual SMAD inhibition; stage 2, astrocyte progenitor induction by a suspension culture; stage 3, astrocyte specification and maturation on a monolayer culture.

(E) Representative images and quantification of induced GFAP+ cells after 52 or 67 days of differentiation. n = 3 independent experiments (with replicate wells) were analyzed. Scale bars, 100 μm.

(F) Induced cells co-expressed GFAP and S100β. Scale bar, 100 μm. Data of this figure are produced by using the TRE3G-NFIA hPSCs (H9). The data are presented as the means ± SEM. *p < 0.05; **p < 0.01 (Student's t test).

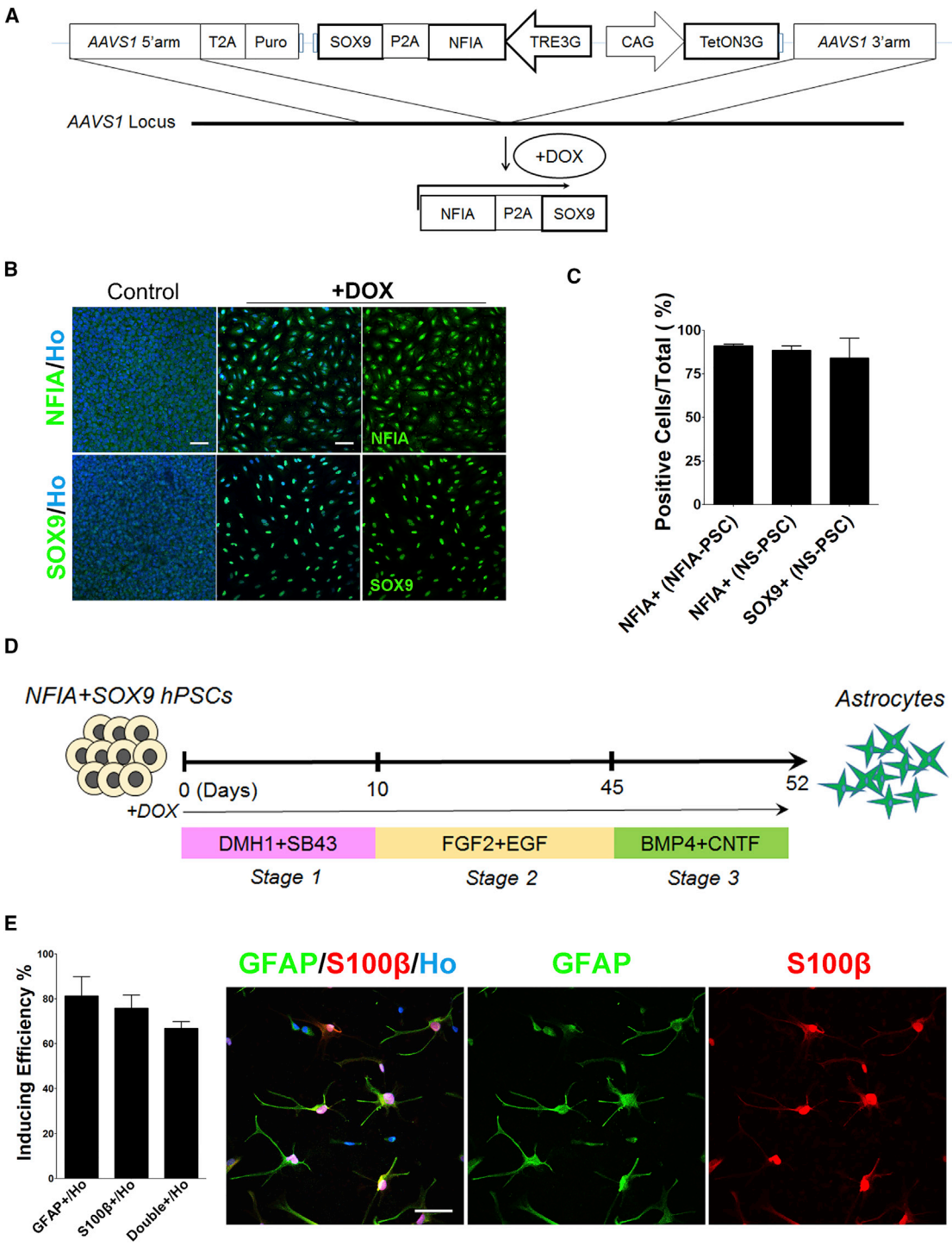

Figure 2. Astrocyte Differentiation Induced by Expression of *NFIA* and *SOX9*

(A) Schematic depiction of the strategy for constructing and targeting TRE3G-*NFIA* + *SOX9* into the AAVS1 locus.

(B) Immunostaining analysis of induced expression of *NFIA* and *SOX9*. Scale bar, 200 μm.

(C) Quantification of positive cells with the induced expression of *NFIA* in NFIA-hPSC line (NFIA+ in NFIA-PSC) and *NFIA* or *SOX9* in NFIA + SOX9 hPSC line (NFIA+ and SOX9+ in NFIA-PSC). PSC colonies from n = 3 replicate cultures were analyzed.

(legend continued on next page)

in a substantially shorter period for generation of astrocytes than that by regular differentiation, which takes 6 months to generate equivalent percentage of GFAP+ cells (Krencik et al., 2011).

To validate the applicability of this strategy, we established two transgenic iPSC lines (WC50 and IMR90) with inducible expression of *NF1A* and *SOX9* using the same approach described above (Figures S2A, S2B, S3A, and S3B). Again, induced astrocytes were efficiently generated from the two iPSC lines (Figures S2C and S3C).

Our time course analysis indicated that the GFAP-expressing astrocytes increase from day 37 to 52 with induction of NF1A or NF1A + SOX9. When we further extended the induction of NF1A and SOX9 for another 60 days, we found that the population of GFAP-expressing astrocytes increased from 80% to 90% (Figure S4A). We noticed that, even at the extended culture, some cells, with expression of S100β and an astrocyte morphology, remained negative or only weakly positive for GFAP (Figure S4A). It has been reported that not all astrocytes express GFAP (Walz and Lang, 1998).

We then asked if the phenotypes of the induced astrocytes are stable when the transgene expression is stopped. We withdrew DOX at day 52 and continued the culture for another 14 days. The induced cells retained their expression of GFAP and S100β (Figure S4B). Furthermore, these induced astrocytes promoted the growth of neurites, including the length and branching (Figure S4C). Thus, the induced cells retain the identity and function of astrocytes. We refer the induced astrocytes from TRE3G-NFIA + SOX9 hPSC lines after a 52-day induction as iAstro.

The iAstro Display Molecular Signatures of Astrocytes

Under our culture condition, the iAstro displayed a star-shaped morphology with delicate processes (Figures 2E and 3A). Immunocytochemical analysis showed that the induced astrocytes co-expressed astrocyte markers, including S100β, ALDH1L1, CD44, and Connexin43 (CX43) (Figure 3A).

If induced transgene expression contributes to the glial differentiation, it is expected that the methylation status of the GFAP promoter is demethylated. Methylation analysis on the GFAP promoter by bisulfite sequencing indicated that the GFAP promoter was methylated in hPSCs but demethylated in the iAstro after induction with NFIA and SOX9 (Figure S4D). This epigenetic change in the GFAP promoter region coincides with transgene-induced glial differentiation.

To further define the identity of the iAstro, we performed RNA-sequencing (RNA-seq) analysis. Hierarchical clustering analysis or principal-component analysis showed that iAstro were placed close to the primary astrocytes but distant from the non-transgene-induced cells, which are mostly neural progenitors (Figures 3B and S4E). Compared with the cells without transgenic induction, the iAstro enriched the expression of astrocyte signature genes, including GFAP, S100β, ALDH1L1, and others (Figure 3C). In contrast, the expression of neuronal genes (e.g., NEFL, NEFM, and NEUN) was suppressed (Figure 3C). Gene ontology analysis further revealed that the upregulated genes after transgenic induction were mainly enriched in cell-cell signaling, extracellular matrix and cell adhesion, inflammatory response, and K+ ion transmembrane transport, whereas the downregulated genes were mainly involved in neuronal fate differentiation, forebrain cell proliferation, synaptic transmission, peptide signaling pathways, neuronal migration, and long-term synaptic potentiation (Figure S4E). Together, these results further validate that the iAstro are indeed astrocytes but not neurons, oligodendrocytes, or neural progenitors.

To determine whether the iAstro retain the astrocyte identity *in vivo*, we transplanted the iAstro after a 52-day induction into the corpus callosum and cerebral cortex of adult severe combined immunodeficiency mice. Three months following transplantation, the grafted astrocytes were detected, as indicated by human-specific GFAP (hGFAP) (Figure 3D). The hGFAP+ cells were larger with elaborated processes compared with the endogenous mouse astrocytes that were labeled by S100β (Figure 3D). Furthermore, the transplanted human cells, as indicated by the expression of human-specific cytoplasm protein Stem121 (Chen et al., 2016), were also positive for SOX9 and CX43 (Figure 3E), markers expressed by mature astrocytes (Roybon et al., 2013; Sun et al., 2017; Wiencken-Barger et al., 2007). Thus, the *in vitro* generated iAstro retain the astrocyte identity *in vivo*.

The iAstro Display Functional Properties of Astrocytes

In vitro, astrocytes are known to support neurite growth. We induced the neurons from EGFP hPSCs (Figure S4F). These resulting EGFP neurons were plated on to the iAstro or alone for 5 days. Measurement of the GFP+ neurites by

(D) Diagram of the facilitated generation of astrocytes by *NFIA* and *SOX9* induction. Stage 1, neural fate commitment by dual SMAD inhibition; stage 2, astrocyte progenitor induction by a suspension culture; stage 3, astrocyte specification and maturation on a monolayer culture.

(E) Representative images and quantification of induced GFAP+/S100β+ cells after 52 days of differentiation. n = 3 independent experiments (with replicate wells) were analyzed. Scale bar, 50 μm. Data in this figure were produced using the TRE3G-NFIA + SOX9 hPSCs (H9). The data are presented as the means ± SEM.

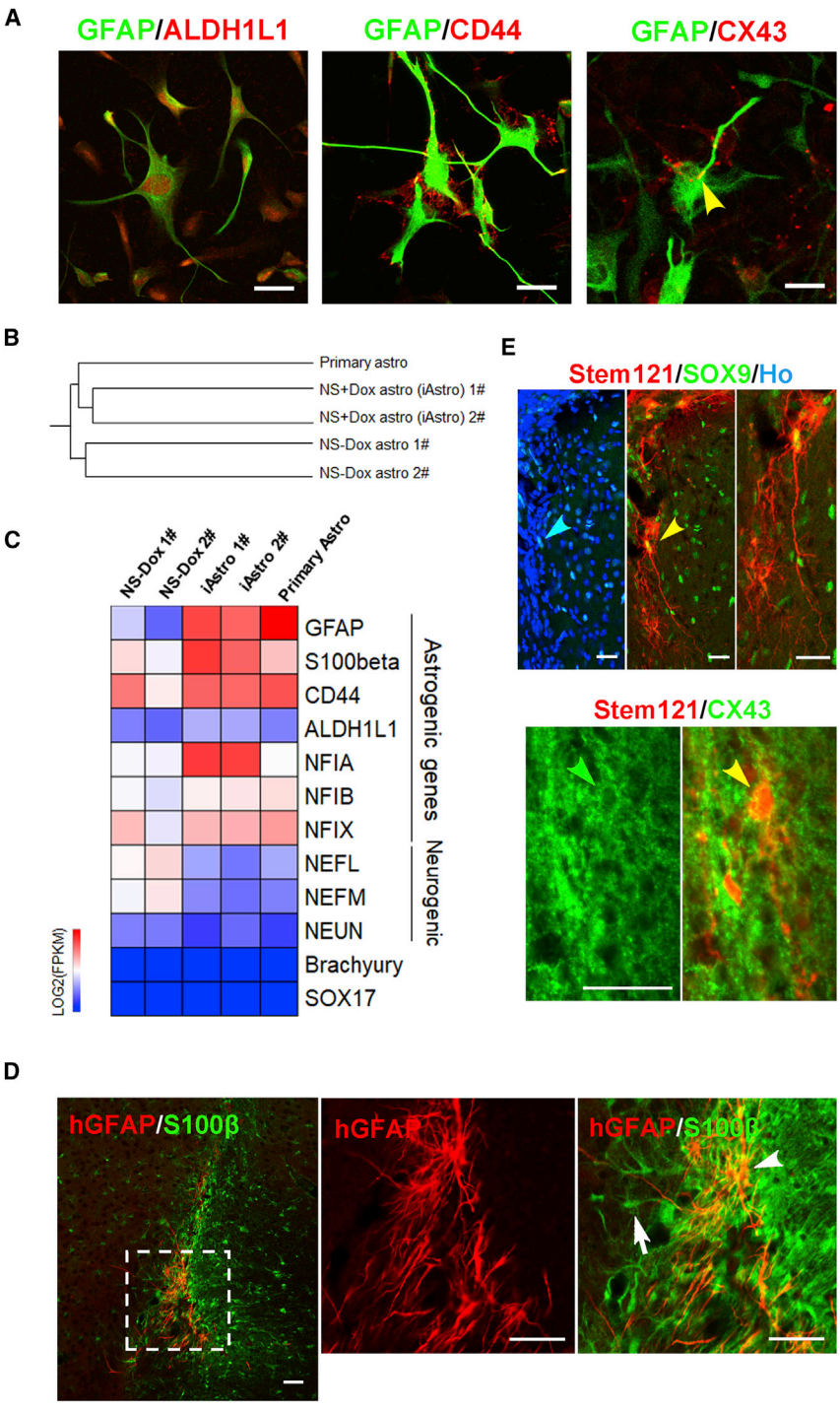

Figure 3. Cellular and Molecular Characterization of iAstro

(A) Representative images of iAstro, showing co-expression of GFAP with ALDH1L1, CD44, and CX43.

(B) Hierarchical clustering analysis of RNA sequencing data from the iAstro, non-transgenically induced cells, and primary astrocytes.

(C) Heatmap profiling of astrogenic and neurogenic genes, mesoderm gene (Brachyury) and endoderm gene (SOX17).

(D) Representative images of transplanted iAstro, showing human-specific GFAP+/S100β+ (hGFAP+/S100β+) and hGFAP−/S100β+ host astrocytes. Arrowhead indicates graft and arrow indicates a host astrocyte. Scale bars, 100 μm.

(E) Representative images of transplanted iAstro (indicated by human-specific cytoplasm marker, Stem121, arrowhead) co-expressing SOX9 and CX43. The area indicated by the yellow arrowhead in the upper row is amplified on the right.

Scale bars, 100 μm. Data in this figure were produced using the TRE3G-NFIA + SOX9 hPSCs (H9).

ImageJ revealed that the neurons co-cultured with the iAstro developed significantly more and longer neurites compared with those without astrocyte co-culture (Figure 4A). A similar phenomenon was observed when using the iAstro derived from the transgenic iPSCs (Figure S4G) or primary fetal human astrocytes (Figure S4H).

Calcium wave propagation across astrocytes is critical for neuron-glia and glia-glia communication (Scemes and Giaume, 2006). When the iAstro derived from TRE3G-NFIA + SOX9 hPSCs (H9) were loaded with Fluor 4 and mechanically stimulated by a pipette, intracellular calcium waves and spikes were instantaneously induced from the

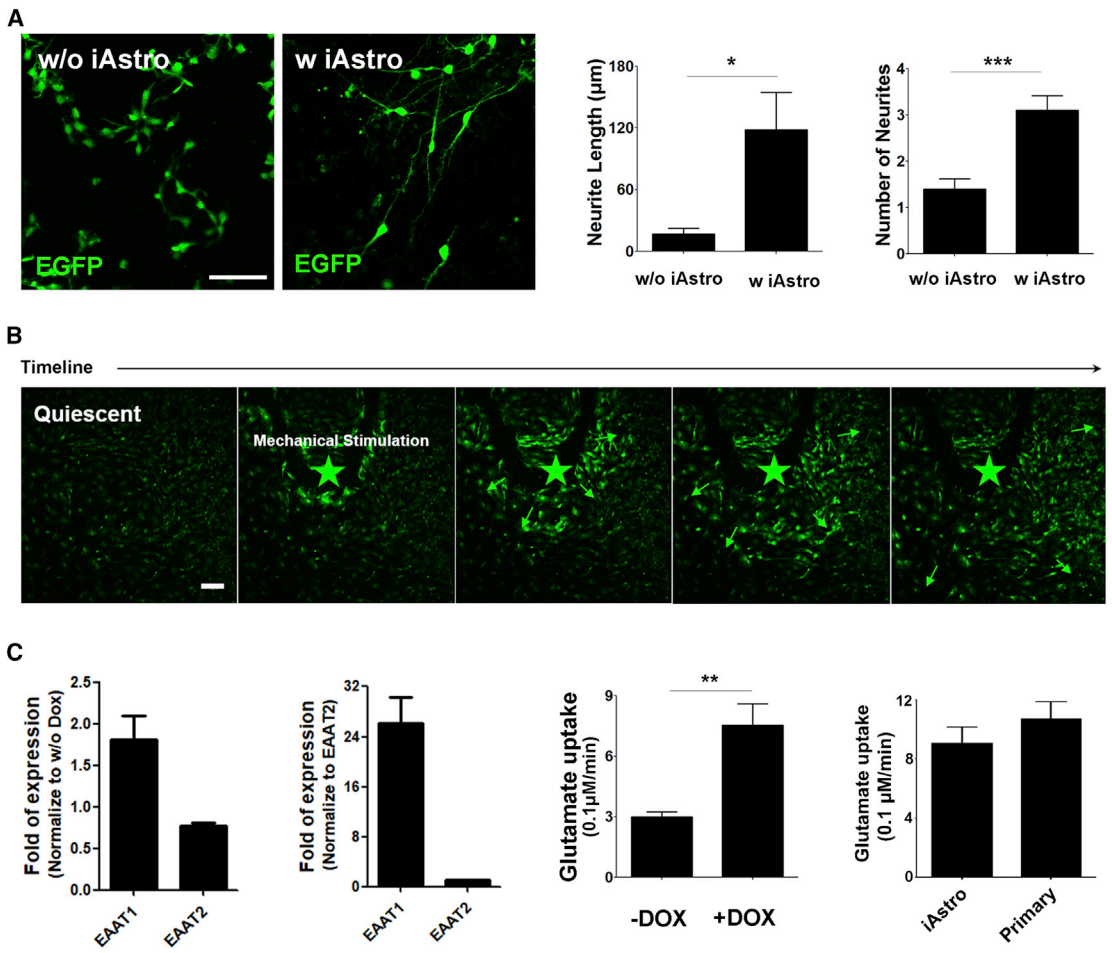

Figure 4. Functional Characterization of iAstro

(A) Quantification of neurite outgrowth from neurons alone or neurons co-culturing with iAstro. n = 3 independent experiments (with replicate wells) were analyzed. Scale bar, 100 μm.

(B) Images of calcium wave propagation over the duration of mechanical stimulation. Asterisk indicates the site of stimulation. Scale bar, 50 μm.

(C) Expression of ETTA1 and ETTA2 in iAstro and the kinetics of cellular uptake of glutamate from the medium. The expression of ETTA1 and ETTA2 are normalized to control cells (w/o DOX). n = 2 replicates for fold expression analysis. n = 8 replicate wells for glutamate uptake analysis and the data are presented as the means ± SEM.

*p < 0.05; **p < 0.01; ***p < 0.001 (Student's t test). Data in this figure were produced using the TRE3G-NFIA + SOX9 hPSCs (H9).

stimulation site (Figure 4B). A similar phenomenon was observed when using the primary fetal human astrocytes (Figure S4H). These calcium waves of iAstro traveled outward to adjacent cells at a speed of 10 ± 1.63 μm/s (Figure S4F), which is faster than primary adult mouse astrocytes *in vivo* (8.6 ± 0.6 μm/s) and slower than primary adult human astrocytes *in vivo* (43.4 ± 4.7 μm/s) (Oberheim et al., 2009).

Astrocytes play a critical role in maintaining the homeostatic brain environment by taking up neurotransmitters. The mRNA expression of glutamate transporters, especially EAAT1, increased significantly after the transgenic induction by DOX (Figure 4C). To determine if the glutamate transporters are functional, we measured glutamate uptake by the iAstro from the culture medium. The iAstro took up glutamate at a rate of 754 ± 214 nM/min. As a comparison, the glutamate uptake by primary astrocytes was 1,066 ± 235 nM/min (Figure 4C). Thus, the iAstro take up glutamate similarly as primary astrocytes.

Fast Generation of Subtype Astrocytes

To determine the optimal window of transcription factor-induced astrocyte differentiation, we titrated the duration of DOX application for inducing iAstro from TRE3G-NFIA + SOX9 hPSCs (H9). We found that the induced transgenic expression in stage 2 (day 10 to 45) was indispensable

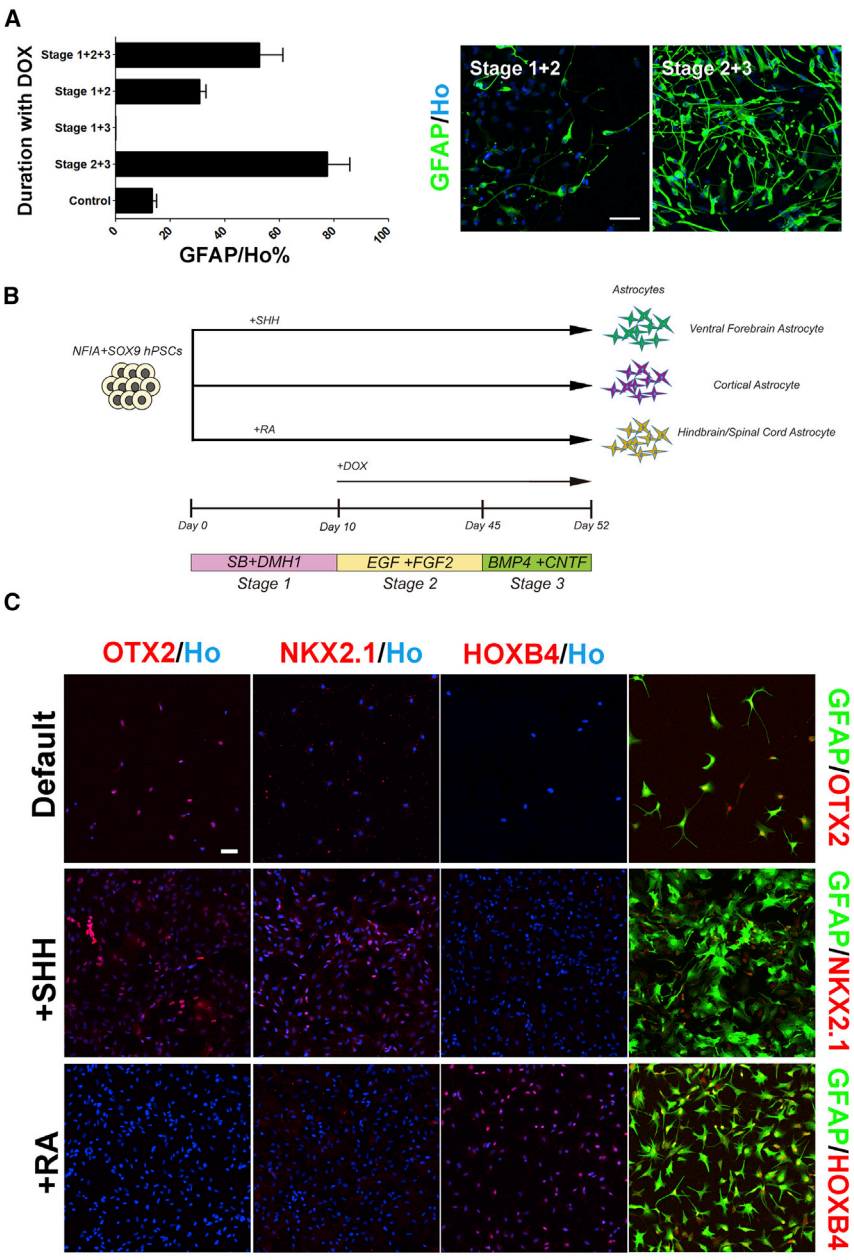

Figure 5. Fast Generation of Region-Specific Astrocyte Subtypes from hPSCs

(A) Optimal window of transcription factor expression for fast induction of astrocytes. n = 3 independent experiments (with replicate wells) were analyzed. Stage 1, neural fate commitment by dual SMAD inhibition; stage 2, astrocyte progenitor induction by suspension culture; stage 3, astrocyte specification and maturation on monolayer culture.

(B) Schematic strategy for fast generation of subtype astrocytes. Examples include fast generation of cortical, ventral forebrain, and hindbrain/spinal cord astrocytes.

(C) Regionally specified cell identity with region-specific markers: OTX2 (forebrain), NKX2.1 (ventral), and HOXB4 (spinal). The astrocyte identity of the induced subtype cells was verified by co-immunostaining with the astrocyte marker GFAP.

Scale bar, 100 μm. Data in this figure were produced using the TRE3G-NFIA + SOX9 hPSCs (H9).

for facilitating astrocyte generation, and the transgenic expression in stage 3 (7-day maturation) further enhanced the efficiency (Figure 5A). In contrast, stage 1 (neuroepithelial induction from day 1 to 10) is dispensable (Figure 5A). This result suggests that NF1A or NF1A plus SOX9 promotes astrocyte differentiation from specified neural progenitors.

In stage 1 of astrocyte differentiation (day 1–10), hPSCs are specified to neuroepithelia which are readily patterned to regional progenitors by morphogens (Li et al., 2005; Tao and Zhang, 2016). We hence asked if regional astrocyte types may be generated at the same speed when the early neuroepithelia are patterned with respective morphogens in stage 1. We differentiated the hPSCs to neuroepithelia in the presence of morphogens for 10 days before induced expression of transgenes for iAstro generation (Figure 5B). In the absence of morphogens, the resulting iAstro (around 70%) were of mostly dorsal forebrain (cortical) identity, as indicated by expression of the forebrain marker OTX2 (Figures 5C and S5). In the presence of ventral patterning morphogen, sonic hedgehog (Shh), a proportion (around 50%) of GFAP+ cells expressed NKX2.1, a ventral forebrain

marker (Figures 5C and S5). In the presence of caudal patterning morphogen retinoic acid (RA), they (>80%) became spinal astrocytes at day 52, as indicated by their co-expression of GFAP and HOXB4 (Figures 5C and S5). Thus, iAstro with different regional identities are generated at the same speed by combining patterning of neuroepithelia and induction of NF1 and SOX9.

DISCUSSION

We have developed a robust method to generate functional astrocytes from hESCs and hiPSCs in 4–7 weeks. This is achieved by CRISPR/Cas9-mediated inducible expression of the gliogenic transcription factors *NFIA* or *NFIA* + *SOX9* in stem cells. The induced cells (or iAstro) exhibit characteristic cellular and functional properties of astrocytes and retain their identity after withdrawal of transgene expression and following transplantation into the mouse brain. Importantly, our method can be extended to generation of astrocyte subtypes in the same time frame by combining regional patterning of neural progenitors and induction of transgenes. This simple and efficient method is substantially faster than the regular differentiation methods mimicking astrocyte development that take 3–6 months (Krencik et al., 2011) and thus helps facilitate the study on human astrocyte biology.

Gliogenesis is a late event during neural development. In humans, it begins at 3 months into gestation and continues for many months. Accordingly, available methods for differentiating hPSCs to astrocytes takes 3–6 months by mimicking the developmental process (Krencik et al., 2011). This is because we lack a non-genetic means to switch the neurogenic progenitors to the gliogenic phase. From the standpoint of developmental biology, gliogenic transcription factors, including *NFIA* and *SOX9*, initiate gliogenesis and maintain the glial identity during neural development (Deneen et al., 2006; Kang et al., 2012; Miller and Gauthier, 2007; Stolt et al., 2003; Tsuyama et al., 2015; Vong et al., 2015). Forced expression of *NFI* and *SOX9* in neuronal progenitor cells *in vivo* or in cultured mouse fibroblasts promotes astrocyte generation (Gaiazzo et al., 2015). By expressing *NFIA* during hPSC neural differentiation, we are now able to generate astrocytes substantially earlier. The addition of *SOX9* further accelerates the differentiation of astrocytes. This is likely due to the coordinated effect of *NFIA* and *SOX9* in initiating gliogenesis (Kang et al., 2012). Indeed, our RNA-seq analysis shows that NF1A and SOX9 repress neuronal differentiation and facilitate glial differentiation. This is also indicated by the methylation assay, showing that the GFAP promoter is demethylated after the transgenic induction, which enables the cells to express the gliogenic gene GFAP during the iAstro differentiation.

Astrocytes in different brain regions exhibit differential properties (Hewett, 2009; Schitine et al., 2015; Sofroniew and Vinters, 2010; Tabata, 2015; Zhang, 2001). We have shown that the iAstro with regional identities can be generated by patterning the early neural progenitors during regular differentiation (Krencik et al., 2011). However, forced expression of neural transcription factors at the beginning of differentiation skips the neural patterning step, resulting in the generation of mature neurons, as demonstrated by *Ngn2*-induced neurons (Zhang et al., 2013). Interestingly, we found that, for iAstro generation, the expression of *NF1A* and *SOX9* is dispensable at the early stage of neural differentiation, suggesting that they act on specified neuroepithelia for astrocyte differentiation. This opens a window of opportunity for us to pattern the early neuroepithelia with respective morphogens for generation of region-specific progenitors before driving the progenitors to iAstro through induction of *NF1A* and *SOX9*. The combination of neural induction/patterning and expression of *NF1A* and *SOX9* enables fast generation of subtypes of functional astrocytes (iAstro).

The functional properties of astroglial subtypes in the adult CNS remain largely undefined (Barres, 2008; Morel et al., 2017; Oberheim et al., 2012). It has been demonstrated that region-specific astrocytes (e.g., cortical or subcortical) selectively promote neurite growth of neurons from the corresponding region (Morel et al., 2017). The gap junction coupling strength appears higher in astrocytes from hippocampus and hypothalamus than those from cerebral cortex and brain stem (Blomstrand et al., 1999). Calcium waves in gray matter protoplasmic astrocytes rely on gap junction coupling to propagate, while fibrous astrocytes of the white matter in the corpus callosum propagate calcium waves depending on ATP (Oberheim et al., 2012). The ability to generate mature astrocyte subtypes from hPSCs will facilitate the investigation of the functional diversity of region-specific astrocytes.

The generation of clonal hPSC lines through CRISPR-mediated transgenesis enables regulation of transgenes in a consistent and reproducible manner, thus producing homogeneous cell populations. This method is simple and can be readily applied to patient iPSCs. The inducible hPSC lines can also be introduced with disease-related mutations for studying the roles of astrocytes in pathogenesis. Hence, the method is advantageous over virus-mediated approaches that involves random transgene integration.

The iAstro exhibit characteristic astrocyte morphology, express astrocytic markers, and maintain their identity after withdrawal of transgenes and transplantation into the mouse brain. Functionally, they resemble primary astrocytes, propagating calcium waves, taking up glutamate, and supporting neurite growth. Therefore, the iAstro are appropriate for studying the biology of human astrocytes

as well as their interactions with surrounding neurons and glia under physiological and pathological conditions. Their ability to survive and integrate into the mouse brain makes it appropriate to analyze the behaviors of the iAstro *in vivo*.

EXPERIMENTAL PROCEDURES

hPSC Culture

HESCs (line H9, passages 20–40) and iPSCs lines (WC50 and IMR90; see also Supplemental Experimental Procedures) were cultured as described previously (Krencik et al., 2011). In brief, cells were passaged weekly by using dispase (1 mg/mL, Gibco) and plating on a monolayer of irradiated mouse embryonic fibroblasts (WiCell). The hPSC culture medium consisted of DMEM/F12 basal medium (Gibco), 20% KnockOut serum replacement (Gibco), 0.1 mM β-mercaptoethanol (Sigma), 1 mM L-glutamine (Gibco), nonessential amino acids (Gibco), and 4 ng/mL FGF-2 (R&D Systems).

Fast Induction of Subtype Astrocytes from Engineered hPSC Lines

TRE3G-*NFIA*/TRE3G-*NFIA* + *SOX9* hPSC lines were established (detailed in the Supplemental Information) and first differentiated to neuroepithelia in the presence of DMH1 (2 μM, Tocris) plus SB431542 (2 μM, Tocris) for 10 days as reported (Chambers et al., 2009; Hu et al., 2010). The cells were digested by EDTA (Gibco) and proceeded into stage 2 induction in suspension in T25 flasks as described above: heparin (1 μg/mL, Sigma) is added in the first week of stage 2 with FGF-2 (10 ng/mL, R&D) and then the cells were cultured with FGF-2 (10 ng/mL, R&D) plus EGF (10 ng/mL, R&D) until stage 3 for maturation. For fast differentiation to cortical astrocytes, the culture was continued without additional regionally patterning factors; for fast differentiation to ventral forebrain astrocytes, Shh (500 ng/mL, R&D Systems) was added (day 0–21); for fast differentiation to spinal astrocytes, RA (500 nM, Tocris) was added (day 0–21). All the groups were treated with DOX (1 μg/mL) from day 11 to induce astrocyte differentiation. After 45 days of induction, the cells were dissociated with Accutase (Chemicon) and attached to Matrigel-coated plates at a density of 5,000–10,000/cm^2 in the presence of BMP4 (10 ng/mL) and CNTF (10 ng/mL) for another 7 days for maturation. For cell transplantation, all procedures were approved by the Animal Care and Use Committee of University of Wisconsin-Madison.

SUPPLEMENTAL INFORMATION

Supplemental Information includes Supplemental Experimental Procedures, five figures, and two tables and can be found with this article online at https://doi.org/10.1016/j.stemcr.2018.08.019.

AUTHOR CONTRIBUTIONS

S.-C.Z. and X.L. conceptualized the study and designed the experiments together. S.-C.Z. supervised the project. X.L. developed the methods. Z.D. provided suggestions and carried out replications in BrainXell. Y.T. performed cell transplantation. R.B. and others provided assistance. L.K. performed glutamate uptake assay. X.L. wrote the manuscript with S.-C.Z.

ACKNOWLEDGMENTS

This work was supported by NIH-NIMH (MH099587 and MH100031), NICHD (HD076892 and U54 HD090256), NIH-NINDS (NS076352, NS086604, and NS096282), the Bleser Family Foundation, the Busta Foundation, and UW2020. X.L. acknowledges a Parkinson's Disease Foundation Postdoctoral Fellowship. S.-C.Z. acknowledges a Steenbock Professorship.

Z.D. and S.-C.Z. are co-founders of BrainXell.

Received: November 29, 2017
Revised: August 27, 2018
Accepted: August 28, 2018
Published: September 27, 2018

REFERENCES

Barres, B.A. (2008). The mystery and magic of glia: a perspective on their roles in health and disease. Neuron *60*, 430–440.

Blomstrand, F., Aberg, N.D., Eriksson, P.S., Hansson, E., and Ronnback, L. (1999). Extent of intercellular calcium wave propagation is related to gap junction permeability and level of connexin-43 expression in astrocytes in primary cultures from four brain regions. Neuroscience *92*, 255–265.

Chambers, S.M., Fasano, C.A., Papapetrou, E.P., Tomishima, M., Sadelain, M., and Studer, L. (2009). Highly efficient neural conversion of human ES and iPS cells by dual inhibition of SMAD signaling. Nat. Biotechnol. *27*, 275–280.

Chen, Y., Xiong, M., Dong, Y., Haberman, A., Cao, J., Liu, H., Zhou, W., and Zhang, S.C. (2016). Chemical control of grafted human PSC-derived neurons in a mouse model of Parkinson's disease. Cell Stem Cell *18*, 817–826.

Deneen, B., Ho, R., Lukaszewicz, A., Hochstim, C.J., Gronostajski, R.M., Anderson, D.J., et al. (2006). The transcription factor NFIA controls the onset of gliogenesis in the developing spinal cord. Neuron *52*, 953–968.

Emdad, L., D'Souza, S.L., Kothari, H.P., Qadeer, Z.A., and Germano, I.M. (2012). Efficient differentiation of human embryonic and induced pluripotent stem cells into functional astrocytes. Stem Cells Dev. *21*, 404–410.

Gaiazzo, M., Giannelli, S., Valente, P., Lignani, G., Carissimo, A., Sessa, A., Colasante, G., Bartolomeo, R., Massimino, L., Ferroni, S., et al. (2015). Direct conversion of fibroblasts into functional astrocytes by defined transcription factors. Stem Cell Reports *4*, 25–36.

Hewett, J.A. (2009). Determinants of regional and local diversity within the astroglial lineage of the normal central nervous system. J. Neurochem. *110*, 1717–1736.

Hu, B.Y., Weick, J.P., Yu, J., Ma, L.X., Zhang, X.Q., Thomson, J.A., Zhang, S.C., et al. (2010). Neural differentiation of human induced pluripotent stem cells follows developmental principles but with variable potency. Proc. Natl. Acad. Sci. USA *107*, 4335–4340.

Iadecola, C., and Nedergaard, M. (2007). Glial regulation of the cerebral microvasculature. Nat. Neurosci. *10*, 1369–1376.

Kang, P., Lee, H.K., Glasgow, S.M., Finley, M., Donti, T., Gaber, Z.B., Graham, B.H., Foster, A.E., Novitch, B.G., Gronostajski, R.M., et al.

(2012). Sox9 and NFIA coordinate a transcriptional regulatory cascade during the initiation of gliogenesis. Neuron *74*, 79–94.

Krencik, R., Weick, J.P., Liu, Y., Zhang, Z.J., and Zhang, S.C. (2011). Specification of transplantable astroglial subtypes from human pluripotent stem cells. Nat. Biotechnol. *29*, 528–534.

Li, X.J., Du, Z.W., Zarnowska, E.D., Pankratz, M., Hansen, L.O., Pearce, R.A., and Zhang, S.C. (2005). Specification of motoneurons from human embryonic stem cells. Nat. Biotechnol *23*, 215–221.

Miller, F.D., and Gauthier, A.S. (2007). Timing is everything: making neurons versus glia in the developing cortex. Neuron *54*, 357–369.

Molofsky, A.V., Krencik, R., Ullian, E.M., Tsai, H.H., Deneen, B., Richardson, W.D., Barres, B.A., Rowitch, D.H., et al. (2012). Astrocytes and disease: a neurodevelopmental perspective. Genes Dev. *26*, 891–907.

Morel, L., Chiang, M.S.R., Higashimori, H., Shoneye, T., Iyer, L.K., Yelick, J., Tai, A., and Yang, Y. (2017). Molecular and functional properties of regional astrocytes in the adult brain. J. Neurosci. *37*, 8706–8717.

Mormone, E., D'Sousa, S., Alexeeva, V., Bederson, M.M., and Germano, I.M. (2014). "Footprint-free" human induced pluripotent stem cell-derived astrocytes for in vivo cell-based therapy. Stem Cells Dev. *23*, 2626–2636.

Oberheim, N.A., Takano, T., Han, X., He, W., Lin, J.H., Wang, F., Xu, Q., Wyatt, J.D., Pilcher, W., Ojemann, J.G., et al. (2009). Uniquely hominid features of adult human astrocytes. J. Neurosci. *29*, 3276–3287.

Oberheim, N.A., Goldman, S.A., and Nedergaard, M. (2012). Heterogeneity of astrocytic form and function. Methods Mol. Biol. *814*, 23–45.

Palm, T., Bolognin, S., Meiser, J., Nickels, S., Träger, C., Meilenbrock, R.L., Brockhaus, J., Schreitmüller, M., Missler, M., Schwamborn, J.C., et al. (2015). Rapid and robust generation of long-term self-renewing human neural stem cells with the ability to generate mature astroglia. Sci. Rep. *5*, 16321.

Qian, K., Huang, C.T., Chen, H., Blackbourn, L.W., 4th, Chen, Y., Cao, J., Yao, L., Sauvey, C., Du, Z., Zhang, S.C., et al. (2014). A simple and efficient system for regulating gene expression in human pluripotent stem cells and derivatives. Stem Cells *32*, 1230–1238.

Robertson, J.M. (2014). Astrocytes and the evolution of the human brain. Med. Hypotheses *82*, 236–239.

Roybon, L., Lamas, N.J., Garcia, A.D., Yang, E.J., Sattler, R., Lewis, V.J., Kim, Y.A., Kachel, C.A., Rothstein, J.D., Przedborski, S., et al. (2013). Human stem cell-derived spinal cord astrocytes with defined mature or reactive phenotypes. Cell Rep. *4*, 1035–1048.

Scemes, E., and Giaume, C. (2006). Astrocyte calcium waves: what they are and what they do. Glia *54*, 716–725.

Schitine, C., Nogaroli, L., Costa, M.R., and Hedin-Pereira, C. (2015). Astrocyte heterogeneity in the brain: from development to disease. Front. Cell Neurosci. *9*, 76.

Scuderi, C., Stecca, C., Iacomino, A., and Steardo, L. (2013). Role of astrocytes in major neurological disorders: the evidence and implications. IUBMB Life *65*, 957–961.

Shaltouki, A., Peng, J., Liu, Q., Rao, M.S., and Zeng, X. (2013). Efficient generation of astrocytes from human pluripotent stem cells in defined conditions. Stem Cells *31*, 941–952.

Sofroniew, M.V., and Vinters, H.V. (2010). Astrocytes: biology and pathology. Acta Neuropathol. *119*, 7–35.

Steinbeck, J.A., and Studer, L. (2015). Moving stem cells to the clinic: potential and limitations for brain repair. Neuron *86*, 187–206.

Stolt, C.C., Lommes, P., Sock, E., Chaboissier, M.C., Schedl, A., Wegner, M., et al. (2003). The Sox9 transcription factor determines glial fate choice in the developing spinal cord. Genes Dev. *17*, 1677–1689.

Sun, W., Cornwell, A., Li, J., Peng, S., Osorio, M.J., Aalling, N., Wang, S., Benraiss, A., Lou, N., Goldman, S.A., et al. (2017). SOX9 is an astrocyte-specific nuclear marker in the adult brain outside the neurogenic regions. J. Neurosci. *37*, 4493–4507.

Tabata, H. (2015). Diverse subtypes of astrocytes and their development during corticogenesis. Front. Neurosci. *9*, 114.

Tao, Y., and Zhang, S.C. (2016). Neural subtype specification from human pluripotent stem cells. Cell Stem Cell *19*, 573–586.

Tcw, J., Wang, M., Pimenova, A.A., Bowles, K.R., Hartley, B.J., Lacin, E., Machlovi, S.I., Abdelaal, R., Karch, C.M., Phatnani, H., Slesinger, P.A., et al. (2017). An efficient platform for astrocyte differentiation from human induced pluripotent stem cells. Stem Cell Reports *9*, 600–614.

Tsuyama, J., Bunt, J., Richards, L.J., Iwanari, H., Mochizuki, Y., Hamakubo, T., Shimazaki, T., Okano, H., et al. (2015). MicroRNA-153 regulates the acquisition of gliogenic competence by neural stem cells. Stem Cell Reports *5*, 365–377.

Ullian, E.M., Sapperstein, S.K., Christopherson, K.S., and Barres, B.A. (2001). Control of synapse number by glia. Science *291*, 657–661.

Vasile, F., Dossi, E., and Rouach, N. (2017). Human astrocytes: structure and functions in the healthy brain. Brain Struct. Funct. *222*, 2017–2029.

Vong, K.I., Leung, C.K., Behringer, R.R., and Kwan, K.M. (2015). Sox9 is critical for suppression of neurogenesis but not initiation of gliogenesis in the cerebellum. Mol. Brain *8*, 25.

Walz, W., and Lang, M.K. (1998). Immunocytochemical evidence for a distinct GFAP-negative subpopulation of astrocytes in the adult rat hippocampus. Neurosci. Lett. *257*, 127–130.

Wiencken-Barger, A.E., Djukic, B., Casper, K.B., and McCarthy, K.D. (2007). A role for Connexin43 during neurodevelopment. Glia *55*, 675–686.

Zhang, S.C. (2001). Defining glial cells during CNS development. Nat. Rev. Neurosci. *2*, 840–843.

Zhang, Y., Pak, C., Han, Y., Ahlenius, H., Zhang, Z., Chanda, S., Marro, S., Patzke, C., Acuna, C., et al. (2013). Rapid single-step induction of functional neurons from human pluripotent stem cells. Neuron *78*, 785–798.

Zhou, S., Szczesna, K., Ochalek, A., Kobolák, J., Varga, E., Nemes, C., Chandrasekaran, A., Rasmussen, M., Cirera, S., et al. (2016). Neurosphere based differentiation of human iPSC improves astrocyte differentiation. Stem Cells Int. *2016*, 4937689.

Stem Cell Reports, Volume *11*

Supplemental Information

Fast Generation of Functional Subtype Astrocytes from Human Pluripotent Stem Cells

Xiang Li, Yezheng Tao, Robert Bradley, Zhongwei Du, Yunlong Tao, Linghai Kong, Yi Dong, Jeffrey Jones, Yuanwei Yan, Cole R.K. Harder, Lindsay Morgan Friedman, Magd Bilal, Brianna Hoffmann, and Su-Chun Zhang

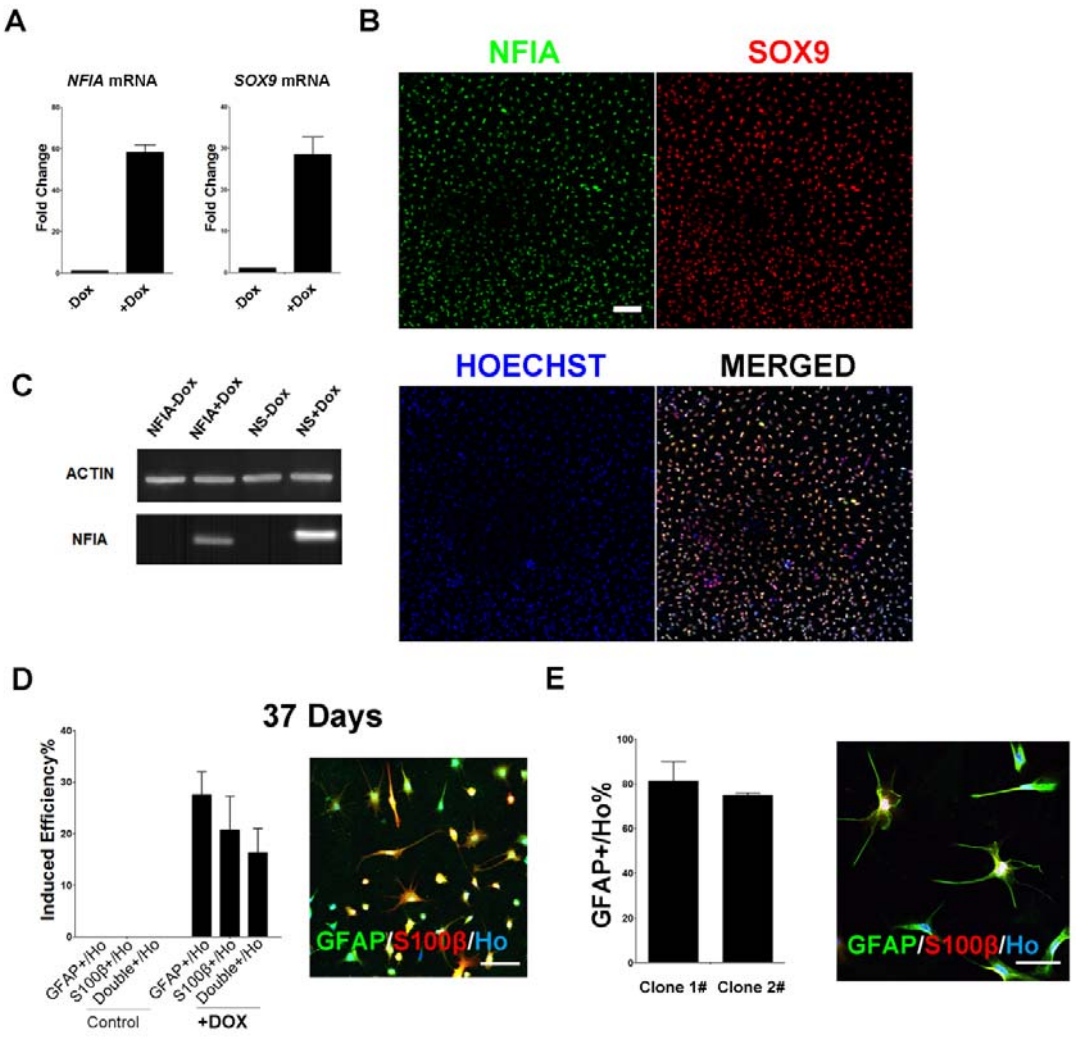

Figure S1. Induced transgene expression facilitate astrocyte generation in hPSCs, related to Figures 1-3.

(A) RT-qPCR analysis of induced *NFIA* and *SOX9* in NFIA+SOX9 hPSCs. **(B)** Co-immunostaining analysis of induced NFIA and SOX9 in NFIA+SOX9 hPSCs. n=3 replicate reactions. Scale bar: 100 μm. **(C)** Western blot analysis of induced NFIA and SOX9 in NFIA+SOX9 hPSCs. Data of this figure is produced by using the TRE3G-NFIA and TRE3G-NFIA+SOX9 hPSCs (H9). **(D)** Quantification and a representative image of induced GFAP+ and S100β+ cells after 30 days of induction and 7 days of maturation. n=3 independent experiments (with replicate wells) were analyzed. Scale bar: 100 μm. **(E)** Quantification and a

representative image of induced efficiency of astrocytes from different clones of TRE3G-*NF1A*+*SOX9* lines. n=3 independent experiments (with replicate wells) were analyzed. Scale bar: 50 μm. Data of this figure is produced by using the TRE3G-NFIA+SOX9 hPSCs (H9).

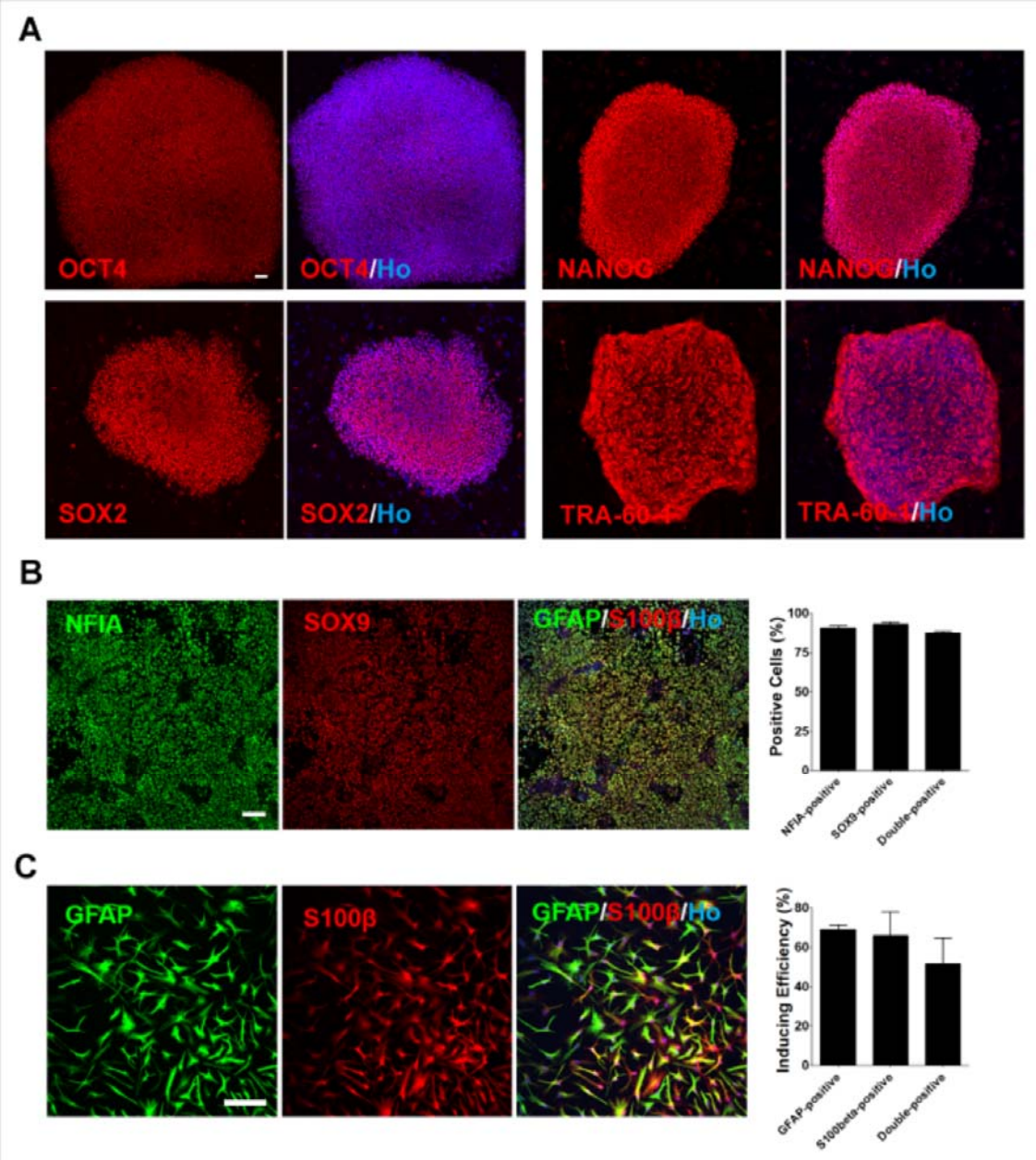

Figure S2. Fast generation of astrocytes from engineered hiPSC lines, related to Figure 2 and 3.

(A) Established TRE3G-*NFIA*+*SOX9* hiPSCs (WC50) expressed typical pluripotency markers: OCT4, NANOG, SOX2, and TRA-1-60. Scale bar: 100 μm. **(B)** Co-immunostaining analysis and quantification of induced expression of *NFIA* and *SOX9*. PSC colonies from n=3 replicate cultures were analyzed. **(C)** Representative images and quantification of induced GFAP+/S100β+ cells after 52 days of differentiation. n=3 independent experiments (with replicate wells) were analyzed. Scale bar: 100 μm. Data of this figure is produced by using the TRE3G-NFIA+SOX9 hiPSCs (WC50).The data is presented as the mean +/− SEM.

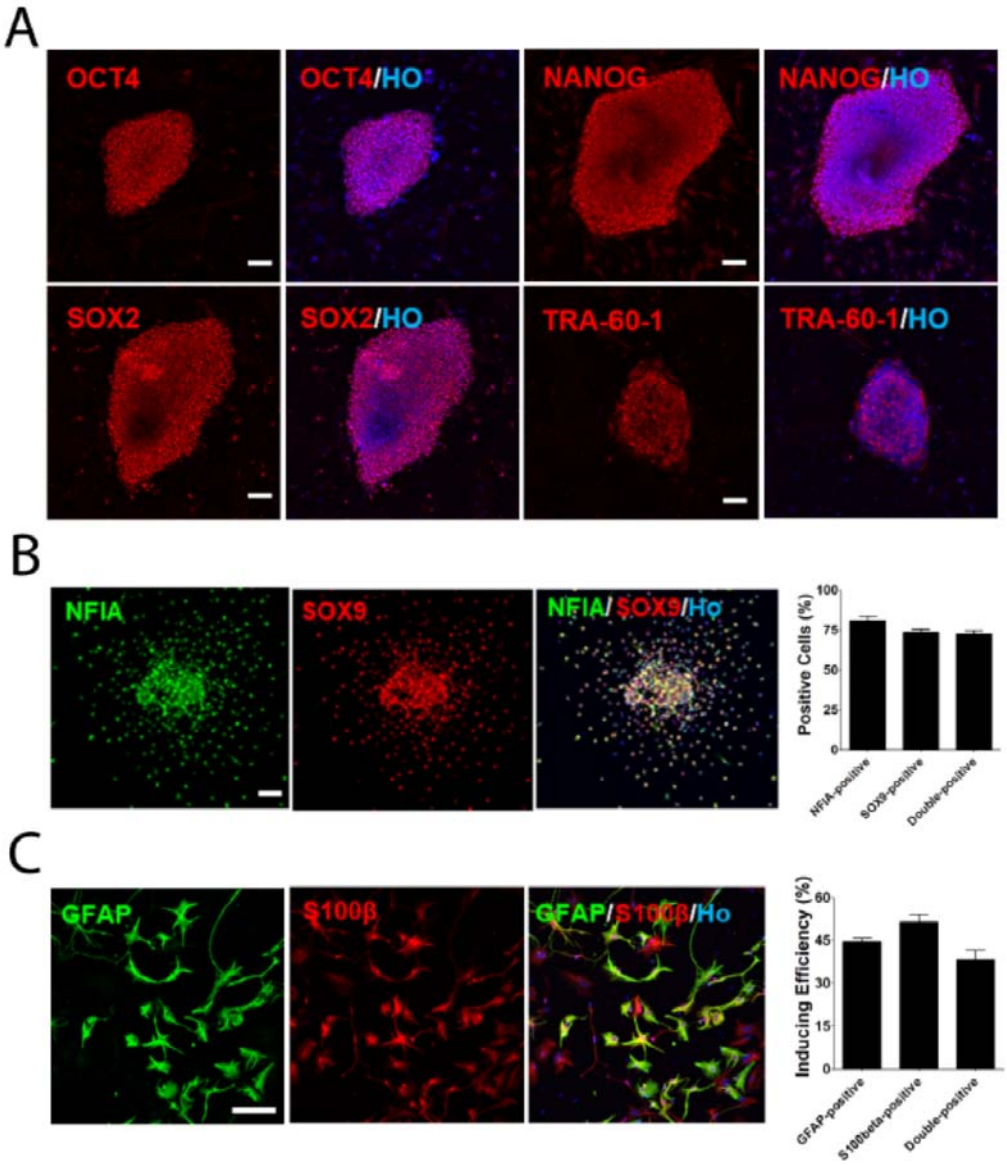

Figure S3. Fast generation of astrocytes from engineered hiPSC lines, related to Figure 2 and 3.

(A) Established TRE3G-*NFIA*+*SOX9* hiPSCs (IMR-90) expressed typical pluripotency markers: OCT4, NANOG, SOX2, and TRA-1-60. Scale bar: 100 μm. **(B)** Co-immunostaining analysis and quantification of induced expression of *NFIA* and *SOX9*. PSC colonies from n=3 replicate cultures were analyzed. **(C)** Representative images and quantification of induced GFAP+/S100β+ cells after 52 days of differentiation. n=3 independent experiments (with replicate wells) were analyzed. Scale bar: 100 μm. Data of this figure is produced by using the TRE3G-NFIA+SOX9 hiPSCs (IMR-90).The data is presented as the mean +/− SEM.

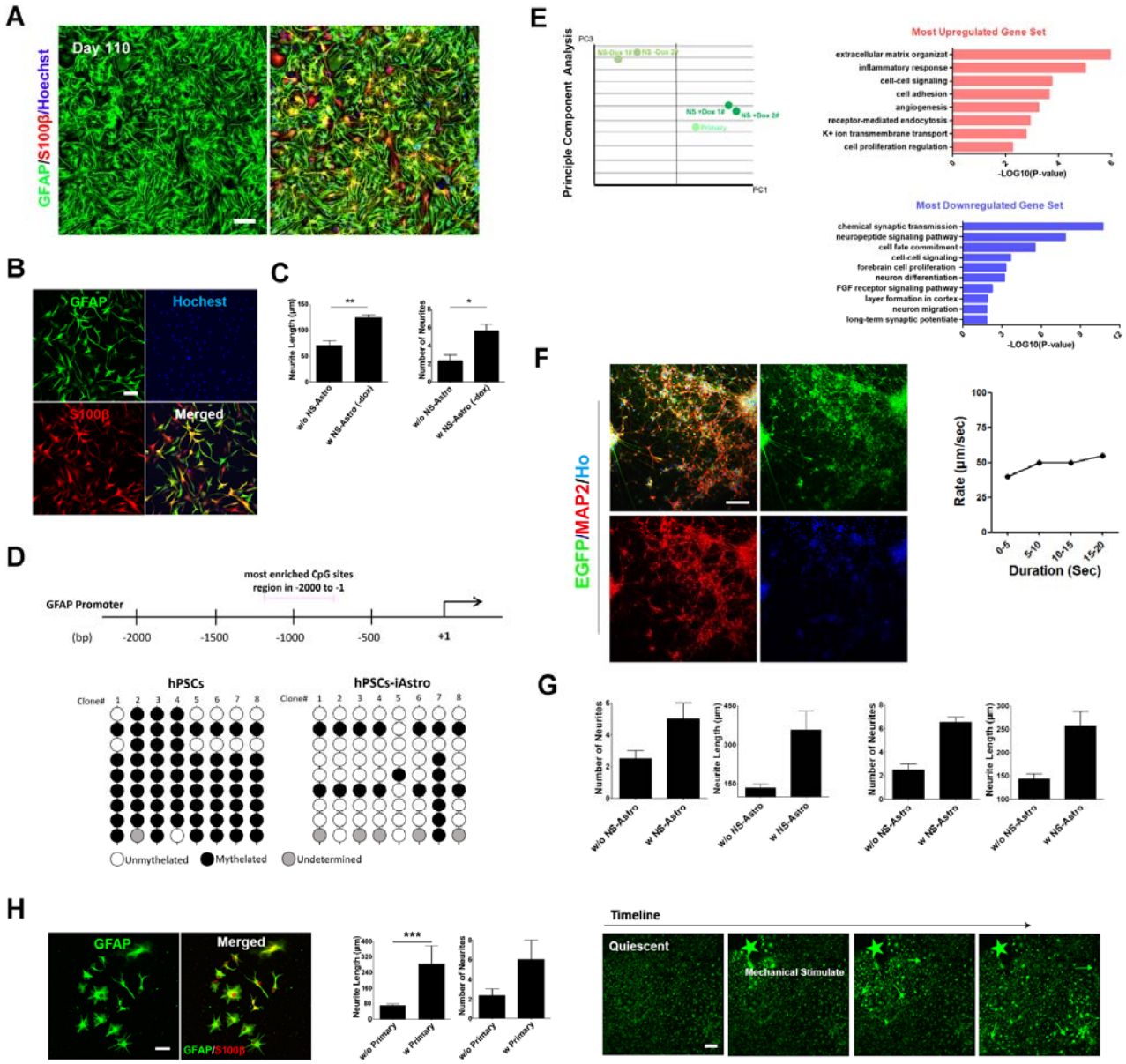

Figure S4. Characterization and comparision of iAstro and primary astrocytes, related to Figure 1-4.

(A) Generation of astrocytes after 110 days of differentiation**.** Data of this figure is produced by using the TRE3G-NFIA+SOX9 hPSCs (H9). **(B)** iAstro retained molecular and functional identity of astrocytes after withdrawing DOX, as indicated by the expression of GFAP+/S100β+. Scale bar: 100 μm. **(C)** iAstro retained functional identity of astrocytes after withdrawing DOX

for 14 days, as indicated by enhanced neurite outgrowth from co-cultured neurons. Data of this figure is produced by using the TRE3G-NFIA+SOX9 hPSCs (H9). n=3 independent experiments (with replicate wells) were analyzed. The data is presented as the mean +/− SEM. *****P<0.05; ******P<0.01 (Student's t-test). **(D)** Methylation analysis of the GFAP promoter. Independent colonies (n=8 for each sample) were selected for analysis. Up: Scheme of the most enriched CpG sites of the GFAP promoter (-2000 to +1bp analyzed; pink line covered region: 9 CpG sites in this region); Down: Bisulfite sequencing results of the CpG site showing most-enriched region in hPSCs (left) and hPSC-iAstro (right). hPSCs: human pluripotent stem cells without differentiation. hPSCs-iAstro: iAstro after 52 days of induction from hPSCs. Data of this figure is produced by using the TRE3G-NFIA+SOX9 hPSCs (H9). **(E)** Additional RNAseq analysis of the iAstro. Left: Principal component analysis (PCA) of iAstro (NS+DOX), differentiated cells without transgene induction by DOX (NS-DOX) and primary astrocytes (PA). Right: GO (Gene Ontology) analysis of the most upregulated genes and downregulated genes after induction. Ten-fold upregulated or downregulated genes (w DOX vs. w/o DOX) were subjected to this analysis. iAstro samples of this figure is generated by using the TRE3G-NFIA+SOX9 hPSCs (H9). **(F)** Additional data for functional characterization of iAstro. Left: Induced EGFP+ neurons from AAVS-CAG-EGFP hPSC line, as indicated by the co-expression of EGFP and MAP2. Scale bar: 100 μm. Right: Quantification of the velocity of calcium wave propagation. The data are presented as the mean +/− SEM. Data of this figure is produced by using the TRE3G-NFIA+SOX9 hPSCs (H9) and AAVS-EGFP H9. **(G)** Quantification of neurite outgrowth from neurons alone or those co-culturing with transgenically induced astrocytes (iAstro). Left two graphs: iAstro from TRE3G-NFIA+SOX9 hiPSC (WC50). Right two graphs: iAstro from TRE3G-NFIA+SOX9 hiPSC (IMR-90). n=3 independent experiments (with replicate wells) were analyzed. The data are presented as the mean +/− SEM. **(H)** Molecular and functional identity of primary astrocytes. Left: Representative image of GFAP+/S100β+ primary human astrocytes. Middle: Neurite outgrowth from neurons co-cultured with primary astrocytes. n=3 independent

experiments (with replicate wells) were analyzed. The data are presented as the mean +/− SEM. ***P<0.001 (Student's t-test). Right: Images of calcium wave propagation in response to mechanical stimulation. Asterisk indicates the site of stimulation. Scale bar: 50 μm.

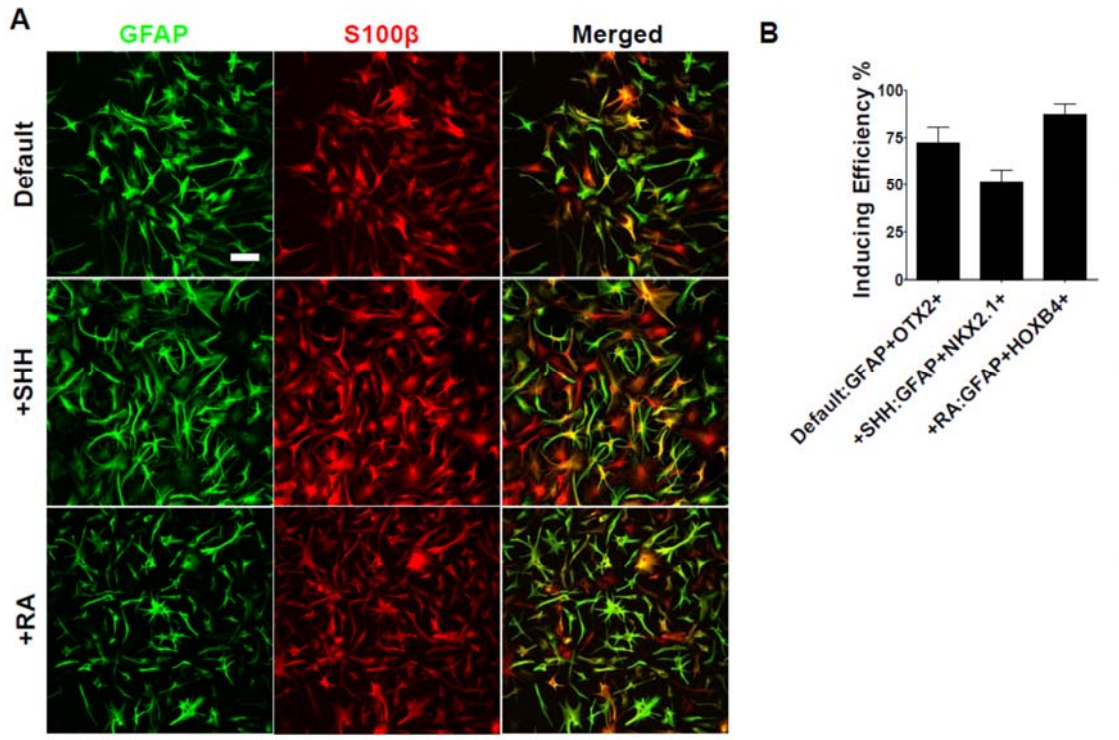

Figure S5. Generation of subtype iAstro, related to Figure 5.

(A) Representative images of GFAP+/S100β+ iAstro with different region-specific identities. Scale bar: 100 μm. **(B)**. Qualification of GFAP+/S100β+ iAstro with region-specific identities, as indicated by region-specific markers. OTX2 (forebrain); NKX2.1 (ventral); HOXB4 (spinal). n=3 independent experiments (with replicate wells) were analyzed. Data of this figure is produced by using the TRE3G-NFIA+SOX9 hPSCs (H9).

SUPPLEMENTAL EXPERIMENTAL PROCEDURES

Generation of AAVS1-TRE3G-*NFIA* and AAVS1-TRE3G-*NFIA*+*SOX9* hPSC lines

The AAVS1-TRE3G-*NFIA* donor plasmid was generated by amplifying the *NFIA* coding sequence from the commercially available cDNA clones (Sequence-Verified cDNA Accession: BC022264 Clone ID: 4270934; #MHS6278-202840360 from Dharmacon.com) and inserting it into the multiple cloning site (MCS) of AAVS1-TRE3G backbone plasmid (Qian et al., 2014). Similarly, the AAVS1-TRE3G-*NFIA*+*SOX9* donor plasmid was generated by inserting the *NFIA* coding sequence without a stop codon into AAVS1-TRE3G backbone. Then we amplified the *SOX9* coding sequence with a P2A flanking sequence from the commercially available cDNA clones (Sequence-Verified cDNA Accession: BC056420 Clone ID: 6200521; #MHS6278-202760124 from Dharmacon.com) and inserted it after *NFIA*. Donor plasmids and sgRNA (Addgene plasmid #41818) targeting the AAVS1 site were used for electroporation. HESCs (H9, from WiCell, passages 20–40) or hiPSCs (WC50: made by BrainXell, Inc, from the fibroblasts of a 60 year's old donor, passages 20-40; IMR90: purchased from WiCell, passage 20-40) were cultured and electroporated, selected by puromycin, picked up as individual colonies and identified by genomic PCR, as we previously reported#(Chen et al., 2015; Chen et al., 2016). Primary human astrocytes (passage 3) were purchased (ScienCell) and cultured according to the manufacture's instruction.

Immunostaining and Quantification

Cells on coverslips/wells were rinsed with PBS and fixed in 4% paraformaldehyde for 20 min. After rinsing with PBS twice, cells were treated with 0.3% Triton for 10 min followed by 10% donkey serum for 1 hour before incubating with primary antibodies overnight at 4 °C. Cells were then incubated for 1h at room temperature with fluorescently-conjugated secondary antibodies (Life Technologies). The nuclei were stained with Hoechst (Ho) (Sigma-Aldrich). Images were taken with a Nikon A1R-Si laser-scanning confocal microscope (Nikon, Tokyo, Japan). The primary antibodies used include the followings: Rabbit anti-GFAP (1:1000, Z033429; Dako); Mouse anti-ALDH1L1 (1:50, Antibodies Incorporated); Mouse anti-GFAP (1:1000, IF03L,

Millipore); Mouse anti-S100β (1:1000, ab11178, Abcam); Rabbit anti-CD44 (1:500, 3578S, Cell Signaling); Rabbit anti-CX43 (1:1000, ab11370, Abcam); Goat anti-OTX2 (1:1000, AF1979, R&D); Mouse anti-NKX2.1 (1:500, MAB5460, Chemicon); Mouse anti-HOXB4 (1:100, I12 anti-Hoxb4, DSHB); Mouse anti-OCT4 (1:500, sc-5279, Santa Cruz); Rabbit anti-SOX2 (1:500, AB5603, Millipore); Rabbit anti-Nanog (1:500, ab21624, Abcam); Mouse anti-TRA-1-60 (1:200, MAB4360, Calbiochem). For quantification, positive cells were counted among the total Hoechst labeled nuclei.

Quantitative reverse transcription polymerase chain reaction (qRT-PCR)

RNA was extracted by the Qiagen RNeasy kit and quantified according to the manufacturer's instruction. 500 ng of RNA was used for reverse transcription using Bio-Rad iScript (1708891) according to the manufacturer's instruction. iTaq universal SYBR Green Supermix (1725124) was used for qPCR reactions (n=3). The qPCR was performed according to the manufacturer's instruction. Values were normalized to GAPDH. The primer sequences were provided in Table S2.

Calcium imaging

Calcium imaging was performed as previously described (Krencik et al., 2011). Induced astrocytes were loaded with Fluor4-AM at a final concentration of 5 μM (ThermoFisher F14201) in HBSS (Gibco) for 30 min. Cells were washed with HBSS twice, switched into phenol-free neurobasal medium (Gibco), and live imaging was taken (n=3). Mechanical stimulation was performed with a flamed glass pipette tip (home-made) manually with a micromanipulator. All imaging was performed on a Nikon A1 confocal using the Nikon Elements software. Data analysis was performed on Nikon Elements software.

Co-culturing neurons with induced astrocytes

The hESCs engineered with AAVS1-CAG-EGFP were differentiated into cortical neuronal progenitors as previously described (Liu et al., 2013). These progenitors (day 21) were digested by EDTA (Gibco) for 1 minute into single cells, centrifuged, and cultured in the neuronal differentiation media alone or on a layer of induced astrocytes (10,000 cells/cm^2) for 5 days, as previously described (Krencik et al., 2011). The cells were subjected to imaging after 5 days of co-culture using Nikon A1R-Si laser-scanning confocal microscope (Nikon, Tokyo, Japan) and the GFP+ neurite length and numbers were counted by ImageJ.

Glutamate clearance assay.

Induced astrocytes were seeded in a 48-well plate at a density of 100,000 cells/well and maintained for four days in the incubator (n=8). The assays were conducted at 37 ºC. Cells were washed three times with pre-warmed HEPES buffered saline solution, after which 5 µM glutamate was added to the culture media, with or without the presence of DL-threo-β-Hydroxyaspartic acid (TBOA; 100 µM), a blocker of excitatory amino acid transporters (EAATs) (Jabaudon et al., 1999; Shigeri et al., 2001; Shimamoto et al., 1998). Ten minutes later, culture media was collected to measure the content of glutamate with a Glutamate Assay Kit (Abcam; Cambridge, MA), following the manufacturer's protocol. Since TBOA inhibits sodium-dependent glutamate transporters, the increase of glutamate levels that was caused by the addition of TBOA was considered EAAT-dependent glutamate uptake.

Methylation Analysis

The prediction of CpG enriched sites of GFAP promoter and the bisulfate primer design were performed with MethPrimer software. The genomic sequences of GFAP promoter (−2000 to +1) (Lee et al., 2008) were downloaded from NCBI and analyzed in the website. Genomic DNA was extracted and treated by bisulfate kit Bisulfite DNA Methylation (Zymo) according to the manufacture's instructions. Methylation-specific PCR primers (Forward:

5’-TTAGAAGTTTAAGGATATAAATGGG-3’; Reverse: 5’-CTAAATCTATCCCTCCAAATCACC-3’) were used to amplify the selected region. Amplified PCR products were gel-purified and cloned into TA-cloning vector for sequencing. Positive colonies (n=8) were randomly chosen for sequencing.

RNAseq

Total mRNA was isolated from cell samples by RNeasy kit (Qiagen) according to the manufacturer’s instructions. RNA sequencing library construction and sequencing was performed as standard HiSeq HighOutput 1×100, by the Biotechnology Center, University of Wisconsin (Sequencing platform information: https://www.biotech.wisc.edu/services/dnaseq). The raw data was analyzed in Galaxy platform following standard protocols available on the website. The RPKM values were used to evaluate the expression levels of genes. The hierarchical clustering and PCA analysis were conducted by Cluster 3.0 and NIA Array platform following standard protocols available on the website. Gene Ontology analysis of the DE genes was performed using the DAVID program following website information available on the website. The accession number for the RNA sequencing data reported in this study is NCBI GEO: GSE118384.

Animal surgery and cell transplantation

Adult SCID mice (100-120 days of age; n=4) were anesthetized with 1%–2% isoflurane mixed in oxygen and received stereotaxic injections of the induced astrocytes in 1μl artificial cerebrospinal fluid (aCSF, Harvard Apparatus) containing Rocki (0.5 μM, EMD Millipore) into the left corpus callosum (CC) and cortex at the following coordinates (AP = +1.5 mm, LM = +1.0 mm, and DV = -2.5 mm for CC, AP = +1.5 mm, LM = +1.0 mm, and DV = -1.5 mm for cortex). About 1×10^5 cells were transplanted into each site.

Immunohistochemistry on brain slices

The animals were sacrificed at the indicated time points after transplantation with an overdose of pentobarbital (250 mg/kg, i.p.) and perfused intracardiacally with 40 ml normal saline, followed by 4% ice-cold phosphate-buffered paraformaldehyde. Then the brains were quickly removed and fixed with 4% paraformaldehyde at 4 °C for about 4 h before immersed sequentially in 20% and 30% PBS-buffered sucrose solution until sunk. Coronal sections (30 μm) were cut with a cryostat (Leica) and kept in the cryoprotectant buffer at -20°C and subjected to immunostaining as described above.

Statistical analysis

Statistical analyses were performed in GraphPad. Significance were calculated with Student's *t*-test. The data are presented as the mean +/− SEM. **P*<0.05; ***P*<0.01; ****P*<0.001.

SUPPLEMENTAL REFERENCES

Chen, Y. et al. (2015). Engineering Human Stem Cell Lines with Inducible Gene Knockout using CRISPR/Cas9. Cell Stem Cell *17*, 233-244.

Jabaudon, D. et al. (1999). Inhibition of uptake unmasks rapid extracellular turnover of glutamate of nonvesicular origin. Proc Natl Acad Sci U S A *96*, 8733-8738.

Lee, Y. et al. (2008). GFAP promoter elements required for region-specific and astrocyte-specific expression. Glia 56: 481-493.

Liu, Y. et al. (2013). Directed differentiation of forebrain GABA interneurons from human pluripotent stem cells. Nat Protoc *8*, 1670-1679.

Shigeri, Y. et al. (2001). Effects of threo-beta-hydroxyaspartate derivatives on excitatory amino acid transporters (EAAT4 and EAAT5). J Neurochem *79*, 297-302.

Shimamoto, K. et al. (1998). DL-threo-beta-benzyloxyaspartate, a potent blocker of excitatory amino acid transporters. Mol Pharmacol *53*, 195-201.

#

TABLE S1. Methods for Efficient Generation of Astrocyte-like Cells from hPSCs*, Related to Figure 1-5.

Ref.	Cell Resource	Method	Efficiency	Time	Molecular Properties	Subtype Identity	Astrocytic Functional Properties			In vivo Characterization
							Glutamate uptake	Support neurons (neurite outgrowth)	Calcium wave	
Krencik et al. 2011	hESCs, hiPSCs	EB, Chemically-defined FGF+EGF→ CNTF+LIF/FBS	~90% GFAP+S100β+	180 days	GFAP, S100β, ALDH1L1, CD44, NF1A -positive	Specifiable for different regions	√	√	√	Survive and retain astrocytic identity.
Emdad et al. 2012	hESCs, hiPSCs	EB, Chemically-defined bFGF+EGF+CNTF	70%~80% GFAP+	35 days	GFAP, A2B5, S100β-positive	×**	×	×	×	×
Shaltouki et al. 2013	hESCs, hiPSCs	EB, Chemically-defined FGF+BMP+CNTF/ FGF+Activin A+Heregulin 1β+IGFI	>80% GFAP+	10+ 35-56 days from PSCs-derived NSCs	GFAP, S100β, CD44 -positive	Mixed	√	√	×	Survive and retain astrocytic identity.
Roybon et al. 2013	hESCs, hiPSCs	Monolayer, Chemically-defined LDN+SB43→ AA+RA+BDNF+GDNF+SHH	~100% S100β+ ~70% GFAP+	>80 days	GFAP, S100β, Vimentin, NF1A, CD44-positive	Spinal Cord	√	×	√	Survive and retain astrocytic identity.
Mormone et al. 2014	hiPSCs	EB, Chemically-defined bFGF+EGF+CNTF	~99% GFAP+	28-35 days	GFAP, A2B5 -positive	×	×	×	×	Survive and retain astrocytic identity.
Palm et al.	hiPSCs	EB	~100%	21+ 45-50	GFAP, S100β,	×	√	×	×	Survive and retain astrocytic identity.

#

#

2015		FCS (serum)	GFAP+/S100β+ /AQP4	days from PSCs-derived NSCs	Vimentin, CD44-positive					
Zhou et al. 2016	hiPSCs	Monolayer/EB SB43+LDN→ FGF+EGF Dissociate	Monolayer: 2%~10% EB:10%~20%	28 days	GFAP, AQP4 -positive	×	×	×	×	×
TCW et al. 2017	hiPSCs	EB; ScienCell commercial astrocyte media	>90% GFAP+/S100β+	14+30 days from PSCs -derived NSCs	GFAP, S100β, Vimentin, ALDH1L1, CD44-positive	Forebrain	√	√	√	×
This study	hESCs, hiPSCs	Monolayer, Chemically-defined NF1A, NF1A+SOX9 DMH1+SB43→ FGF+EGF→BMP4+CNTF	~80% GFAP+S100β+	30-60 days	GFAP, S100β, ALDH1L1, CD44, CX43 -positive	Specifiable for different regions	√	√	√	Survive and retain astrocytic identity.

***** Astrocyte purification/generation methods from long-term cultured 3D spheroids (usually taking hundreds of days) were not included and compared in this Table.

******Undetermined in the publication.

Table S2. Primers used for real-time qPCR. Related to Figure 1 and Figure S1.

GENE NAME	FORWARD (5' TO 3')	REVERSE (5' TO 3')	APPLICATION
NFIA	ACAGGTGGGGTTCCTCAATC	GTGGGACGCTGCAACTTTT	real-time qPCR
SOX9	ACCCGCACTTGCACAACG	GGTGGTCCTTCTTGTGCTG	real-time qPCR

#